Fabrication of Tin Sulphide and Emerging Transition Metal Di-chalcogenides by CVD

Chung-Che Huang[1], Ghadah A. Alzaidy[1], Nikolaos Aspiotis[1], Ed C. Weatherby[1], Shuncai Wang[2], John C. Walker[2], Zheng Jiang[2] and Daniel W. Hewak[1]*

[1]Optoelectronics Research Centre, University of Southampton, Southampton, SO17 1BJ, U.K.
[2]Engineering and the Environment, University of Southampton, Southampton, SO17 1BJ, U.K.
*Email: cch@orc.soton.ac.uk

Introduction

Graphene, one of the most important two dimensional (2D) materials, has been attracting increasing interest and new applications in nano-scale electronic and photonic applications. The zero bandgap of graphene, however, has restricted its use in some optoelectronic applications. Recently, transition metal di-chalcogenides (TMDCs) such as MoS_2, $MoSe_2$, WS_2 and WSe_2 have become a noteworthy complimentary material to graphene sharing many of its properties [1-3]. They may however offer properties that are unattainable in graphene since TMDCs offer tuneability through both composition and number of layers, allowing a bandgap transition from indirect to, with the single layer, direct. The use of chalcogenide thin films such as $CuInGaSe_2$ and CdTe in solar cells have been commercialized but the search for low cost, low toxicity and earth abundant high efficiency absorbing materials remains under investigation. Tin mono-sulphide, a p-type semiconductor with a band gap of ~1.3 eV, has attracted great interest for the use as an absorber layer in chalcogenide thin film solar cells due to its desirable properties [4]. In addition, TMDCs are now emerging in the thin film photovoltaic [5] and photo-catalyst [6] applications. The current challenge in the fabrication of TMDC thin films is to form an industrially scalable and controllable deposition methodology. Chemical vapour deposition (CVD) technology has the advantage of offering conformal, scalable, and controllable thin film growth on a variety of different substrates [7]. Here we report our recent developments in CVD technology for Sn-S and 2D TMDCs materials, in particularly MoS_2 and WS_2. These chalcogenide thin films have been deposited by CVD onto various substrates at room temperature then annealed at different temperatures with the aim of optimizing the properties of the thin films to achieve the required phase. These annealed thin films were further characterized with SEM, TEM, EDX, XRD, Raman, UV-VIS-NIR, and photoluminescence spectroscopy. The preliminary results of these CVD-grown chalcogenide thin films show great promise for energy applications.

Experimental

The CVD apparatus for chalcogenide thin film deposition is shown schematically in **Fig.** 1. The precursors used for Sn-S, Mo-S, and W-S were $SnCl_4$, $MoCl_5$, and WCl_6 respectively. During the deposition process, the precursor was kept in a bubbler at room temperature, and precursor vapour was delivered by an argon carrier gas through a mass flow controller (MFC) to the quartz CVD reaction tube. The reactive gas, H_2S, was delivered through a second MFC. The argon gas flow rates for delivering the precursor and the H_2S gas were typically set at 100 sccm and 200 sccm respectively. This CVD preparation methodology of chalcogenide thin films is easily combined with conventional lithography techniques thus allowing patterned structures on a range of substrates with the distinct advantage that initial deposition takes place at room temperature.

The CVD-grown Sn-S thin films were annealed at 350 °C with H_2S gas to achieve SnS phase while the Mo-S/W-S thin films were first annealed with H_2 and H_2S mixture gases at 500 °C to remove Cl atoms, followed by an additional annealing process with H_2S gas at 900 °C to convert MoS_2/WS_2.

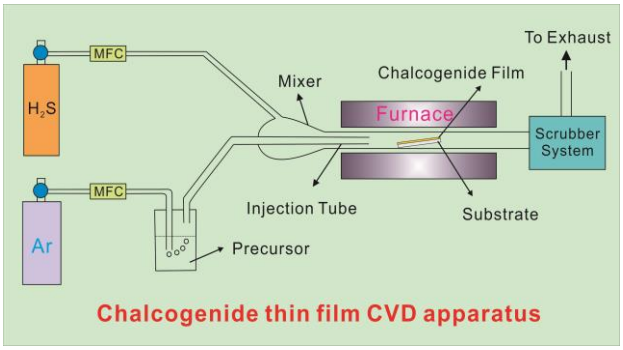

Figure 1. Schematic diagram of the CVD apparatus for chalcogenide thin film deposition.

Results and Discussion

1. Fabrication of Sn-S by CVD. $SnCl_4$ precursor was used to react with H_2S gas to form Sn-S thin films on various substrates including soda-lime glass, SiO_2/Si, and sapphire at room temperature by the CVD system shown in **Fig.** 1. The composition of the CVD as-deposited Sn-S thin film, $Sn_{37}S_{34}Cl_{29}$, was determined by energy dispersive X-ray spectroscopy (EDX) analysis, which revealed that as-deposited Sn-S thin films contained unreacted Cl atoms. These as-deposited Sn-S thin films have been further characterized with X-ray diffraction (XRD) and micro-Raman. From the XRD analysis shown in **Fig**. 2(a), the chlorine contaminated Sn-S was in amorphous phase and from the Raman spectrum shown in **Fig.** 3(a), these Sn-S thin films were predominantly in SnS_2 phase.

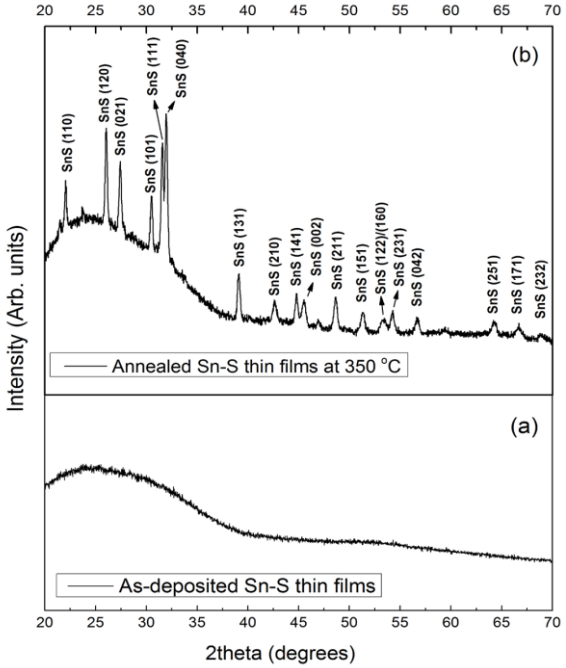

Figure 2. XRD patterns of (a) room temperature as-deposited Sn-S thin film and (b) annealed Sn-S thin film at 350 °C.

The as-deposited Sn-S thin film samples were then annealed at five different temperatures 200, 250, 350, 400, 450 °C in a tube furnace with a gas mixture of argon and H_2S in order to achieve SnS phase which is a p-type semiconductor with a band gap of ~1.3 eV. From the **Fig.** 2(b), the XRD patterns of annealed Sn-S thin films at 350 °C have completely matched with the crystal structure of Herzenbergite SnS (JCPDS No. 39-0354, lattice parameters of a = 4.3291 Å, b = 11.1923 Å, and c = 3.9838 Å).

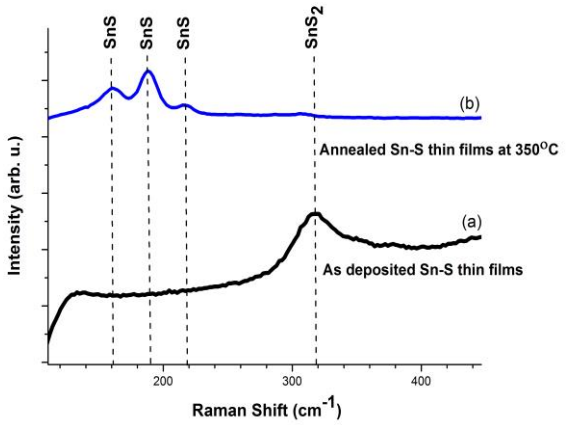

Figure 3. Raman spectra of (a) room temperature as-deposited Sn-S thin film and (b) annealed Sn-S thin film at 350 °C.

From the XRD pattern shown in **Fig.** 2(b) and Raman spectrum shown in **Fig.** 3(b), the Tin mono-sulphide can be achieved by our CVD technique for the deposition at room temperature followed by the anneal process at 350 °C. A typical SEM image (**Fig.** 4) of annealed SnS thin film on soda-lime glass substrate revealed the polycrystalline nature of the Sn-S thin film.

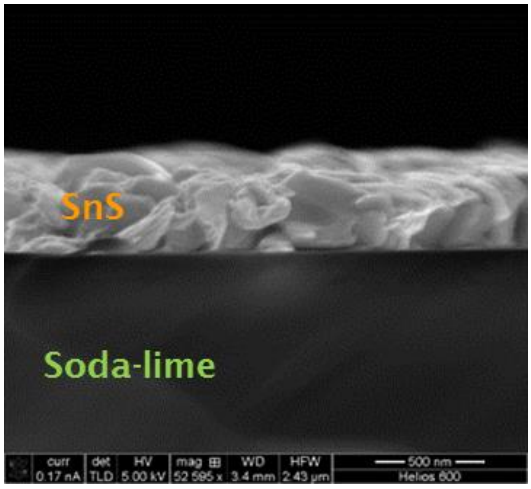

Figure 4. A typical SEM image of 350 °C annealed CVD grown Sn-S thin film on soda-lime substrate.

This is an important milestone in the preparation of low cost, low toxicity and earth abundant high efficiency absorbing material for the future photovoltaic application.

2. Fabrication of TMDCs by CVD. $MoCl_5/WCl_6$ precursors were used to react with H_2S gas to form Mo-S/W-S thin films on various substrates including quartz glass, SiO_2/Si, and sapphire at room temperature by the CVD system shown in Fig. 1. The composition of the CVD as-deposited Mo-S thin films, $Mo_{26}S_{61}Cl_{13}$, was determined by energy dispersive X-ray spectroscopy (EDX) analysis, which revealed that as-deposited Mo-S thin films contained excess sulfur and a small proportion of unreacted Cl atoms. In order to transform the $Mo_{26}S_{61}Cl_{13}$ to a pure MoS_2 thin film, a two-step annealing process was developed. A typical sample of single and few layers MoS_2 with dimensions of 40mm by 100 mm is shown in **Fig.** 5 that has been fabricated using this scalable CVD process [7].

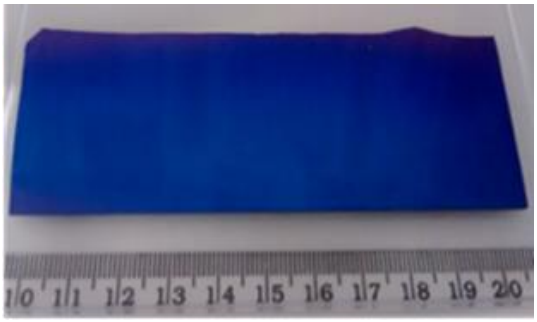

Figure 5. A photo of CVD grown MoS_2 on SiO_2/Si substrate

A Jeol 3010 Transmission electron microscope (TEM) measurement on a FIB (Zeiss NVision40) prepared lamella also revealed ordered crystalline MoS_2 grown on c-plane sapphire, confirming the XRD measurements. Five periodically arranged layers of MoS_2 oriented along the (0001) direction of sapphire (**Fig.** 6) and no amorphous region was observed confirming the crystalline nature of the MoS_2.

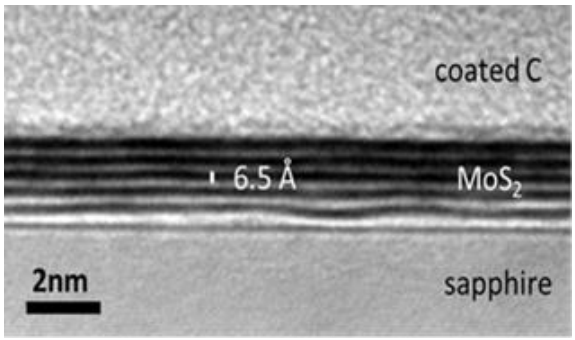

Figure 6. TEM image of CVD grown MoS_2/sapphire substrate

A RENISHAW Raman microscope equipped with a CCD camera was used to characterize these annealed CVD-grown MoS_2/WS_2 thin films on SiO_2/Si, SiO_2 and sapphire substrates. A 532 nm laser was used to excite the sample and the Raman spectra were measured from 150 cm^{-1} to 550 cm^{-1} with a resolution of 0.1 cm^{-1}. The Raman spectra of these CVD-grown MoS_2/WS_2 thin films are shown in **Fig.** 7 which reveals two characteristic MoS_2 Raman peaks, E^1_{2g} in-plane phonon mode at 382.7 cm^{-1} and A_{1g} out-of-plane phonon mode at 405.0 cm^{-1}. The WS_2 Raman peaks are more

complicated with the 532 nm excitation laser. Apart from the A_{1g} at 416.6cm^{-1} and E^1_{2g} at 351.4cm^{-1}, some second order Raman peaks from phonon couplings with a nonzero momentum are also found, however this second order peaks can be reduced by using shorter wavelength laser.

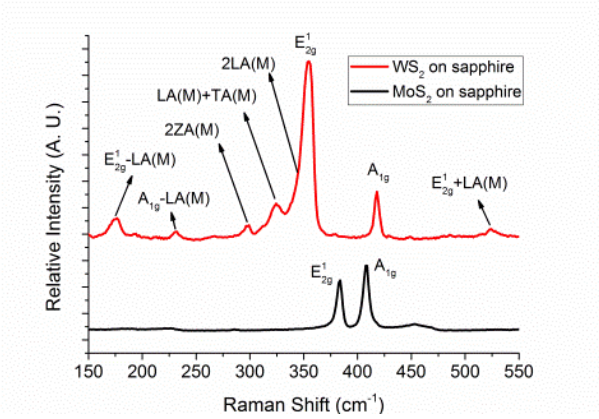

Figure 7. Raman spectra of CVD-grown MoS_2/WS_2 thin films on sapphire substrates

X-ray diffraction measurements of the MoS_2 grown on c-plane sapphire also confirmed the conclusions drawn from the Raman analysis. With a grazing incidence (2°), a sharp MoS_2 (0002) diffraction peak was observed at $2\theta = 14.5$, shown in **Fig.** 8a. In addition, MoS_2 higher order (0004) and (0008) diffraction peaks were observed with the symmetric Bragg-Brentano geometry setup (**Fig.** 8b). The different spectra, which show a dependence on the XRD measurement geometry, confirmed that the ultrathin MoS_2 film grown on c-plane sapphire was highly oriented along the stacking axis. In order to further investigate the crystal nature of MoS_2 thin films grown by this APCVD technique, a 30nm thick MoS_2 thin film on c-plane sapphire substrate was prepared for pole figure measurements. Data was obtained using a Rigaku Smart lab X-ray diffractometer. Two peaks were chosen from the MoS_2 JCPDS file (00-037-1492) provided by the International Centre for Diffraction Data (ICDD).

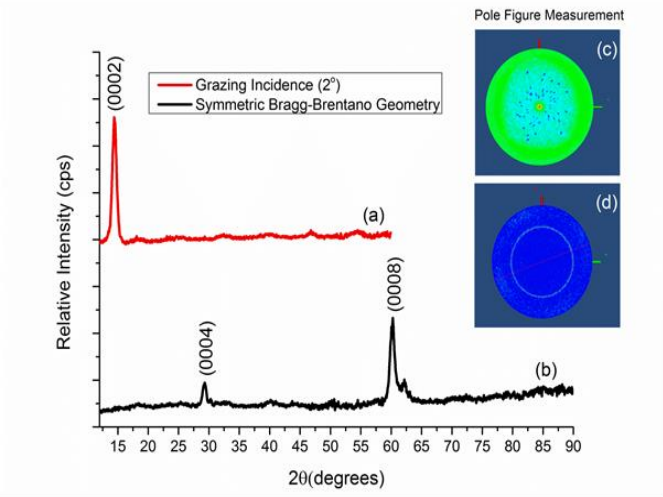

Figure 8. X-ray diffraction patterns of CVD grown MoS_2 thin film on c-plane sapphire substrate with (a) grazing incidence (2°) setup, (b) symmetric Bragg-Brentano geometry setup (c) pole figure measurement of the 002 plane (d) pole figure measurement of the 103 plane.

The two peaks are present at 14.38 degrees and 39.54 degrees, corresponding to the 002 and 103 crystal planes respectively. These peaks were chosen because they show the highest intensities in general diffractograms. In addition, by comparing the pole figure measurements of two intersecting planes we can deduce the nature of film growth. The pole figure measurement of the 002 plane, Fig. 8c, shows a high intensity at 90 degrees (normal to surface), which means the layers formed homogeneously in the z-plane and are equidistant from one another (consistent d-spacing). The instrumentation peak broadening prevented a Scherrer analysis of the minimum crystal grain size; the grains are much larger than 130 nm-the lower size limit that can be reliably measured with this XRD system. The pole figure measurement around the (103) planes, see Fig. 8d, shows diffraction rings and not individual peaks, which indicates a quasi-epitxial growth of large domains with in-plane rotation.

A Cary 500 UV-VIS-NIR spectrometer was used to determine the optical properties of these MoS_2 thin films. Two MoS_2 direct-gap transitions can be identified from the absorption spectrum in the range of 1.2 - 2.4 eV.[8] The UV-VIS-NIR absorption spectra of a 15 nm thick MoS_2 thin film grown on silica substrate (**Fig.** 9a) and 10 nm thick MoS_2 thin film grown on c-plane sapphire substrates (**Fig.** 8b) have confirmed these two direct-gap transitions. In **Fig.** 8a, peak A and peak B were found at 1.81 eV and 1.96 eV respectively, whereas in **Fig.** 9b, peak A and peak B were found at 1.85 eV and 2.00 eV respectively. The band gap of the 10 nm thick CVD grown MoS_2 thin film grown on c-plane sapphire was ~1.85 eV which agrees with the measurement made on chemically exfoliated MoS_2 thin films.[2, 9] However, these two direct-gap transitions in the poly-crystalline MoS_2 on silica substrate shifted to lower energy by 0.4 eV compared to those of single crystalline MoS_2 on c-plane sapphire substrate. These results suggest that polycrystalline MoS_2 thin films display a strain related shift in the bandgap. [10]

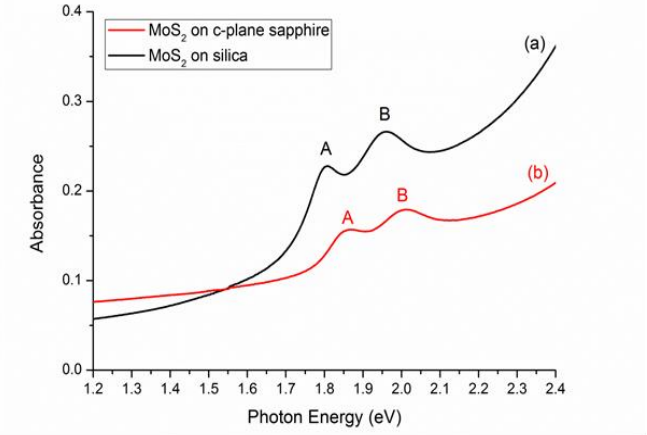

Figure 9. UV-VIS-NIR absorbance spectra of CVD grown MoS_2 thin films on (a) silica substrate (b) c-plane sapphire substrate.

In addition, the photoluminescence (PL) emission from the CVD grown MoS_2 on c-plane sapphire substrate was measured from

550nm to 740nm using the RENISHAW Raman microscope. This PL spectrum shown in Fig. 10 revealed the excitonic peak A and peak B at 675nm (1.84 eV) and 625nm (1.98 eV) respectively. These results are also in agreement with UV-VIS-NIR measurements.

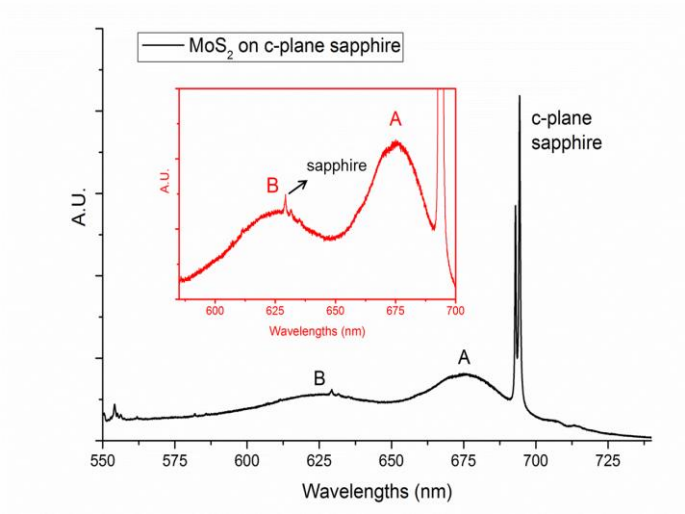

Figure 10. Photoluminescence spectrum of CVD grown MoS_2 thin film on c-plane sapphire substrate (zoom in peak A and peak B in the inset figure).

The MoS_2/WS_2 thin films grown using this CVD process display intriguing optical and electronic properties and they show great promise for energy applications.

Conclusions

In conclusion, SnS and TMDCs, such as MoS_2/WS_2, thin films have been successfully deposited on SiO_2/Si, quartz glass, and sapphire substrates by CVD at ambient temperature, followed by an annealing process. These annealed SnS, MoS_2, and WS_2 thin films have been characterized with SEM, EDX, micro-Raman, XRD, TEM, UV-VIS-NIR, and photoluminescence spectrometry. Key optical and electronic properties of CVD grown chalcogenide thin films have been determined. This CVD process is scalable and can be easily incorporated with conventional lithography as the deposition is taking place at room temperature. These APCVD grown chalcogenide thin films show great promise for energy applications.

Acknowledgement

The authors would like to acknowledge the technical assistance of Mr. Ed Weatherby and Mr. Chris Craig. This work was funded by the Engineering Physical Sciences Research Council through EPSRC Centre for Innovative Manufacturing in Photonics and Zepler Institute Research Collaboration Stimulus Fund 2014/15. The authors also thank Dr. Pier Sazio, Dr. Harold Chong and Dr. Sakellaris Mailis for helpful discussions, Dr. Mark Light for the assistance of XRD measurement, and the access to Zeiss NVision 40 FIB-SEM for TEM lamella sample preparation by Dr. John Walker in Southampton Nanofabrication Centre.

References

(1) Wang Q.; Kalantar-Zadeh K.; Kis A.; Coleman J. N.; and Strano M. S., *Nat. Nanotechnology*, **2012**, *7*, 699.
(2) Radisavljevic B.; Whitwick M. B.; and Kis A., *ACS Nano*, **2011**, *5*, 9934.
(3) Geim A. K.; and Grigorieva I. V., *Nature*, **2013**, *499*, 419.
(4) Sinsermsuksakul P.; Chakraborty R.; Kim S. B.; Heald S. M.; Buonassisi T.; and Gordon R. G., *Chem. Mater.*, **2012**, *24* (23), 4556.
(5) Tsai M.-L.; Su S.-H; Chang J.-K; Tsai D.-S; Chen C.-H.; Wu C.-I.; Li L.-J.; Chen L.-J.; and He J.-H., *ACS Nano*, **2014**, *8* (8), 8317.
(6) Li Y.; Li Y.-L.; Araujo C. M.; Luo W.; and Ahuja R., *Catal. Sci. Technol.*, **2013**, *3*, 2214.
(7) Huang C.C.; Al-Saab F.; Wang Y.; Ou J.Y.; Walker J.C.; Wang S.; Gholipour B.; Simpson R.E.; and Hewak D.W., *Nanoscale*, **2014**, *6*, 12792.
(8) Mak K. F.; Lee C.; Hone J.; Shan J.; and Heinz T. F., *Phys. Rev. Lett.*, 2010, 105, 136805.
(9) G. Eda, H. Yamaguchi, D. Voiry, T. Fujita, M. Chen, M. Chhowalla, "Photoluminescence from chemically exfoliated MoS2", Nano Lett., **2011**, *11*, 5111.
(10) Feng J.; Qian X.; Huang C.; and Li J., *Nature Photonics*, **2012**, *6*, 866.